62-0; **12d**, 132017-63-1; **13a**, 132017-64-2; **13b**, 132017-65-3; **13d**, 132017-66-4; **14**, 10349-38-9; **15a**, 61831-48-9; **15b**, 132017-67-5; **15d**, 132017-68-6; **16a**, 30160-18-0; **16b**, 132017-69-7; **16d**, 132017-70-0; **17**, 24075-35-2; **18a**, 132017-71-1; **18b**, 132017-72-2; **19a**, 132017-73-3; **19b**, 132017-74-4; **30a**, 132017-75-5; **30a** (debromo derivative), 14636-27-2; **30b**, 132017-76-6; **30b** (debromo derivative), 132017-78-8; **31**, 132017-77-7; $PhCH{=}CH(CH_2)_3I$, 132017-79-9; 2-benzylcyclopentanone, 2867-63-2.

Absorbance, Light Intensity, Mass Transfer, and Sampling Time Effects in a Proposed Mechanism for the Photolysis of Phenyl Azide

Guillermo Terrones[†] and Arne J. Pearlstein*[,‡]

Contribution from the Department of Aerospace and Mechanical Engineering and Department of Chemical Engineering, The University of Arizona, Tucson, Arizona 85721.
Received December 7, 1989. Revised Manuscript Received October 25, 1990

Abstract: In the concentrated phenyl azide solutions in which Costantino et al. have reported apparent quantum yields for azide disappearance (ϕ_{-PhN_3}) on the order of 1000 and interpreted their results in terms of a branching-chain mechanism, the optical penetration depth is sufficiently small that the proposed chain-initiation reaction is effectively confined to a very thin layer near the front optical window. Simple calculations show that this layer is sufficiently thin that diffusive mass transfer is important on the time scale of the experiments. On the basis of the mechanism of Costantino et al., we develop and investigate a model consisting of three nonlinear integro-partial differential equations accounting for the nonuniform light absorption, photochemical kinetics, and diffusive mass transfer. The dependence of ϕ_{-PhN_3} on initial azide concentration is shown to be in good qualitative agreement with experiment. The model predicts that the apparent quantum yield is sometimes a strong function of the time at which the reaction mixture is sampled. The relatively simple mechanism proposed by Costantino et al. is consistent with their results, as well as the more recent measurements of Liang and Schuster, in which quantum yields in excess of unity were not observed. In terms of the proposed branching-chain mechanism, the apparent discrepancies between the results of Costantino et al. and Liang and Schuster can be attributed to the use of different light intensities.

In large part due to their use as photolabeling agents, polymerization initiators, and cross-linking agents,[1] there has been considerable recent interest in the photochemistry of aryl azides,[2-9] with special emphasis on the photolysis of phenyl azide. Recently, additional interest has developed in this area due to the fact that the photolysis can lead to the formation of poly(1,2-azepines). When the process is performed through a photomask, the oxidation products of the poly(1,2-azepines) can form a patterned, semiconducting polymeric film[10] of interest in microelectronics manufacture.

In dilute solution, the photodecomposition of phenyl azide at 254 nm proceeds with a quantum yield (for the disappearance of phenyl azide) of about 0.5, in both nonpolar ($\phi_{N_2} = 0.53 \pm 0.10$ in hexane at 25 °C and 0.52 ± 0.10 in a matrix of methylcyclohexane at 77 K)[11] and polar ($\phi_{-PhN_3} = 0.57 \pm 0.19$ in deoxygenated acetonitrile)[2] solvents.

Recently, Costantino et al.[2] have reported that, in the photolysis of concentrated ($>10^{-3}$ M) solutions of phenyl azide in acetonitrile, ϕ_{-PhN_3} may exceed 10^4. They have proposed a branching-chain mechanism involving triplet nitrene radicals, a chain-initiation step (1), a chain-branching step (2), and two chain-termination steps (3 and 4), which is proposed to be valid over the entire range of azide concentration. Jenkins et al.[3] have conducted a mechanistic study of the photodecomposition of several substituted phenyl azides in the presence of various triplet sensitizers as well as a known singlet quencher and have concluded that the intermediate nitrene in (1-4) is a triplet species.

$$PhN_3 \xrightarrow{h\nu} PhN + N_2 \quad (1)$$

$$PhN + PhN_3 \rightarrow [X] \rightarrow 2PhN + N_2 \quad (2)$$

$$PhN + PhN_3 \rightarrow Ph{-}N{=}N{-}Ph + N_2 \quad (3)$$

$$2PhN \rightarrow Ph{-}N{=}N{-}Ph \quad (4)$$

Recently, Liang and Schuster[9] and Li et al.[12] have questioned the validity of the mechanism (1-4) at high azide concentrations. Using time-resolved infrared and ultraviolet absorption spectroscopy to monitor the concentration of 1,2-didehydroazepine following flash photolysis of phenyl azide, Li et al. have proposed an alternative mechanism, in which the singlet excited azide undergoes intersystem crossing to an excited triplet azide or loses N_2 to form a singlet nitrene. The latter species may undergo either a reversible isomerization to 1,2-didehydroazepine or intersystem crossing to a triplet nitrene, a species which may also result from loss of N_2 by triplet azide. Li et al. propose that azobenzene is formed by dimerization of two triplet nitrenes and that 1,2-didehydroazepine either reacts with azide to give a (presumably polymeric) tarry substance or is converted to triplet nitrene by a process not involving isomerization to singlet nitrene. At low

* To whom correspondence should be addressed at Department of Mechanical and Industrial Engineering, University of Illinois at Urbana-Champaign, 1206 West Green St. Urbana, IL 61801.
† Department of Aerospace and Mechanical Engineering.
‡ Department of Aerospace and Mechanical Engineering and Department of Chemical Engineering.

(1) Breslow, D. S. In *Azides and Nitrenes*; Scriven, E. F. V., Ed.; Academic: New York, 1984.
(2) Costantino, J. P.; Richter, H. W.; Lee Go, C. H.; Waddell, W. H. *J. Am. Chem. Soc.* **1985**, *107*, 1744-1747.
(3) Jenkins, R. F.; Waddell, W. H.; Richter, H. W. *J. Am. Chem. Soc.* **1987**, *109*, 1583-1584.
(4) Waddell, W. H.; Lee Go, C. *J. Am. Chem. Soc.* **1982**, *104*, 5804-5805.
(5) Lee Go, C. H.; Waddell, W. H. *J. Am. Chem. Soc.* **1984**, *106*, 715-718.
(6) Lee Go, C.; Waddell, W. H. *J. Org. Chem.* **1983**, *48*, 2897-2900.
(7) Feilchenfeld, N. B.; Waddell, W. H. *Chem. Phys. Lett.* **1983**, *98*, 190-194.
(8) Leyva, E.; Platz, M. S.; Persy, G.; Wirz, J. *J. Am. Chem. Soc.* **1986**, *108*, 3783-3790.
(9) Liang, T.-Y.; Schuster, G. B. *J. Am. Chem. Soc.* **1987**, *109*, 7803-7810.
(10) Meijer, E. W.; Nijhuis, S.; van Vroonhoven, F. C. B. M. *J. Am. Chem. Soc.* **1988**, *110*, 7209-7210.
(11) Reiser, A.; Marley, R. *Trans. Faraday Soc.* **1968**, *64*, 1806-1815.
(12) Li, Y.-Z.; Kirby, J. P.; George, M. W.; Poliakoff, M.; Schuster, G. B. *J. Am. Chem. Soc.* **1988**, *110*, 8092-8098.

0002-7863/91/1513-2132$02.50/0

azide concentrations, the overall rate of the didehydroazepine–azide reaction is reduced relative to the rate at which 1,2-didehydroazepine is converted to triplet phenylnitrene.

When these two proposed mechanisms are evaluated, it is important to understand clearly the implications and kinetic predictions of each. For concentrated phenyl azide solutions, Costantino et al.[2] analyzed their mechanism (1–4) and made the standard steady-state approximation for the intermediate PhN, obtaining the relation

$$\phi_{-PhN3} = \Phi_1 + 2(k_2^2 - k_3^2)[PhN_3]^2\frac{N_0}{4k_4I_{abs}} \qquad (5)$$

where Φ_1 is the quantum yield of the primary process (1), N_0 is Avogadro's number, $I_{abs} = I_0(1 - 10^{-A_0})/V_0$ is the volumetric rate of light absorption, k_2, k_3, and k_4 are bimolecular rate constants, and V_0 and A_0 are the volume and absorbance, respectively, of the irradiated solution.

Unfortunately, (5) is based on the assumption of a uniform initiation rate (1) and a uniform distribution of the intermediate nitrene species within the irradiated volume. As discussed in the following text, the absorbance of the concentrated solutions studied by Costantino et al.[2] was in most cases greatly in excess of unity. Thus, the photochemical reaction (1) is effectively confined to a thin layer near the front optical window of the reaction cell. As a result, one might also expect the nitrene distribution within the reaction cell to be highly localized. In that event, the rate of the chain-branching step would be highly nonuniform. Moreover, the layer within which the initiation process would be confined would be sufficiently thin for diffusive mass transfer to be important for a time scale on the order of the duration of the experiment. The potential importance of these nonuniformities for a mechanism involving a biradical termination step (4) and in which the product azobenzene may act as a light-absorbing screen is evident.

We have thus undertaken a numerical investigation of the effects of nonuniform light absorption and diffusive mass transfer on the photodecomposition of concentrated phenyl azide solutions in acetonitrile, in the context of the mechanism proposed by Costantino et al.[2] The dependence of the quantum yield on the irradiation time has also been investigated. We focus here on the experiments performed by Costantino et al.[2] under "deoxygenated" conditions, restricting consideration to the relatively simple mechanism (1–4) with three reacting and two light-absorbing species. Our model includes the kinetics corresponding to the proposed mechanism (1–4) of Costantino et al.,[2] molecular diffusion, and light absorption by phenyl azide and the product, azobenzene. It gives rise to a system of three coupled integro-partial differential equations that are solved numerically by a finite difference procedure. The results are in good qualitative agreement with those of Costantino et al.[2] over the entire range of initial $[PhN_3]$ investigated by them as well as with the more recent experiments of Liang and Schuster,[9] in which quantum yields in excess of unity were not observed.

Importance of Absorbance and Mass-Transfer Effects

We present in this section a simple quantitative estimate of the importance of diffusive transport in the experiments of Costantino et al.[2]

The experiments of Costantino et al.[2] were conducted in rectangular cuvettes with flat optical surfaces.[13] Thus, the transmission and absorption of light by the solution may be described by a simple form of Beer's law, with the intensity at time t and a distance x from the optical window at which the light enters the reactor being given by

$$I'(x,t) = I_0' \exp[-A(x,t) \ln 10] \qquad (6)$$

where I_0' is the incident light flux (photons cm^{-2} s^{-1}) and the absorbance is defined by

$$A(x,t) = \int_0^x [\epsilon_1 C_1(y,t) + \epsilon_3 C_3(y,t)]\, dy \qquad (7)$$

(13) Waddell, W. H.; Richter, H. W. Private communication.

Table I. Initial Absorbance, Irradiation Times, and Quantum Yields of Disappearance of Phenyl Azide in Deoxygenated Acetonitrile[1]

$[PhN_3]$, M	$A(L,0)$	t_{irr}, s	ϕ_{-PhN_3}	F
1.40×10^{-5}	0.140	30	0.31	0.035
1.57×10^{-5}	0.157	30	0.42	0.036
1.60×10^{-5}	0.160	30	0.47	0.036
2.13×10^{-5}	0.213	30	0.66	0.038
2.30×10^{-5}	0.230	30	0.46	0.038
2.30×10^{-5}	0.230	30, 60, 90	0.56	0.038
1.29×10^{-4}	1.29	25	0.97	0.090
1.34×10^{-4}	1.34	30	0.70	0.093
1.60×10^{-4}	1.60	60	1.52	0.107
1.60×10^{-4}	1.60	90	1.48	0.107
1.60×10^{-4}	1.60	30	1.70	0.107
1.60×10^{-4}	1.60	60	1.83	0.107
2.30×10^{-4}	2.30	60	2.11	0.148
3.00×10^{-4}	3.00	25	3.49	0.187
3.96×10^{-4}	3.96	30	1.59	0.239
3.00×10^{-3}	3.00×10^{1}	25	5.25×10^{1}	0.874
3.21×10^{-3}	3.21×10^{1}	30	1.59×10^{1}	0.891
4.15×10^{-3}	4.15×10^{1}	30	5.23×10^{1}	0.943
5.24×10^{-3}	5.24×10^{1}	30	4.04×10^{1}	0.973
2.76×10^{-2}	2.76×10^{2}	30	2.94×10^{2}	1.000
3.00×10^{-2}	3.00×10^{2}	25	3.00×10^{2}	1.000
5.65×10^{-2}	5.65×10^{2}	30	5.63×10^{2}	1.000
7.73×10^{-2}	7.73×10^{2}	30	6.79×10^{2}	1.000
1.29×10^{-1}	1.29×10^{3}	30	3.58×10^{3}	1.000
6.14×10^{-1}	6.14×10^{3}	30	1.29×10^{4}	1.000
7.22×10^{-1}	7.22×10^{3}	30	1.53×10^{4}	1.000

In (7), C_1 and C_3 are the concentrations of phenyl azide and azobenzene, respectively, ϵ_1 and ϵ_3 are the corresponding molar absorptivities, and the concentration of the intermediate nitrene, denoted by C_2, has been assumed to be sufficiently small so that its absorption may be neglected. We note that at 254 nm the molar absorptivities are[5,14] $\epsilon_1 = 10^4$ M^{-1} cm^{-1} and $\epsilon_2 = 10^3$ M^{-1} cm^{-1} and that the conversion of PhN_3 is very small (said[2] to be less than 3%). The initial absorbance can be calculated on the basis of ϵ_1 and the initial concentration of phenyl azide. In the experiments of Costantino et al.,[2] the optical path length was 1 cm.[13] For the molar absorptivity at 254 nm of azobenzene, which acts as an inner filter during the photolysis, we use $\epsilon_3 = 3.6 \times 10^3$ M^{-1} cm^{-1} based on ref 15. This corresponds to a mixture of approximately 90% (*E*)-azobenzene and 10% (*Z*)-azobenzene. A more refined calculation would account for the fact that (*E*)-azobenzene appears[6] to be the isomer formed in (1–4), and the well-known photoisomerization of (*E*)- and (*Z*)-azobenzenes (see ref 6 for further references). For the purposes of our simulation, neglecting the dynamics of the isomeric distribution of the azobenzene species will affect the calculation only by changing the importance of the inner filter effect associated with light absorption by azobenzene.

On the basis of these data, the initial absorbances (shown in Table I) have been calculated for the experiments of Costantino et al.[2] The results show that $A(L,0)$ is always in excess of 0.1, and for the experiments in which the measured quantum yield ϕ_{-PhN_3} exceeds 10, $A(L,0)$ exceeds 30. The absorbance provides a useful measure of the nonuniformity of the light absorption and chain-initiation rates within the reaction vessel; high values indicate that both will be highly localized near the front optical window of the cuvette.

Table I also shows the duration of each experiment[13] and, at $t = 0$, the fraction F of the total light absorption that occurs within the first 0.27 mm of the front optical window. This length is the characteristic diffusion-length scale $L_{diff,1} = (D_1 t_f)^{1/2}$ for an experiment of duration $t_f = 25$ s with an estimated diffusion coefficient of 2.97×10^{-5} cm^2 s^{-1} for PhN_3 in acetonitrile (based on the Scheibel, Lusis-Ratcliff, and Reddy–Doraiswamy correlations[16]). Thus, in all cases in which ϕ_{-PhN_3} exceeds 10, most

(14) Reiser, A.; Bowes, G.; Horne, R. J. *Trans. Faraday Soc.* **1966**, *62*, 3162–3169.

(15) *Sadtler Handbook of Ultraviolet Spectra*; Sadtler Research Laboratories: Philadelphia, 1979; p 254.

(and in the majority of the cases, essentially all) of the absorption and chain initiation occur near the front optical surface within a layer sufficiently thin for diffusive mass-transfer effects to be important, even on the relatively short time scale of the experiments.

Importance of Sampling Time

For the mechanism proposed by Costantino et al.[2] a serious problem in determining the quantum yield of disappearance of phenyl azide at high concentrations arises from the fact that the quantum yield must start at Φ_1 (see Analytical Results) and ultimately decay to zero (owing to the continuing light absorption by azobenzene long after the reaction is essentially complete). At intermediate times, ϕ_{-PhN_3} may attain values on the order of 10^3 in the experiments of Costantino et al.[2] and in our simulations. Thus, the time at which the quantum yield is measured is very important.

Mathematical Model

We describe in this section a relatively simple mathematical model that includes the phenomena relevant to the proposed mechanism of Costantino et al.[2] with the exception of buoyancy-driven convection. As discussed previously,[17] the illumination of an absorbing fluid by a beam directed in any direction other than parallel or antiparallel to the gravity vector must necessarily give rise to buoyancy-driven fluid motion. In the experiments of Costantino et al., the irradiating beam was horizontal,[13] and the importance of the resulting convection is likely to be accentuated by the highly nonuniform nature of the light absorption, described previously.

Variations of the concentration and light intensity in directions perpendicular to that of the irradiating beam are also neglected. In fact, the irradiation in the experiments of Costantino et al.[2] was not uniform over the 1 cm × 4 cm face of the front optical surface, being confined to a rectangular slit 1 mm × 4 mm. The characteristic time scale for diffusion to replenish the reaction volume will be on the order of $t_{diff,1} = (1\ mm)^2/D_1$, where the width of the illuminated slit is taken as the characteristic length. This gives a time on the order of 300 s, which is considerably longer than any of the experiments.

Finally, although buoyancy-driven convection in this geometry is likely to effect significant reductions in the spatial nonuniformities, the confinement of the initiation reaction to extremely thin layers at the highest optical densities (vide supra) is unlikely to be ameliorated by convection. This is because in liquids the concentration and thermal boundary layers giving rise to the buoyancy force are inherently thinner than the momentum boundary layers associated with the ensuing free convection.

Thus, in order to elucidate the primary aspects of the light absorption, photochemical and secondary reaction kinetics, and diffusive mass transfer associated with the proposed mechanism, convection will be neglected, and it will be assumed that the only significant variations occur along the optical path.

We begin with conservation equations

$$\frac{\partial C_1}{\partial t} = D_1\frac{\partial^2 C_1}{\partial x^2} - \Phi_1\alpha_1 I'(x,t)C_1 - (k_2 + k_3)C_1C_2 \quad (8a)$$

$$\frac{\partial C_2}{\partial t} = D_2\frac{\partial^2 C_2}{\partial x^2} + \Phi_1\alpha_1 I'(x,t)C_1 + (k_2 - k_3)C_1C_2 - 2k_4C_2^2 \quad (8b)$$

$$\frac{\partial C_3}{\partial t} = D_3\frac{\partial^2 C_3}{\partial x^2} + k_3C_1C_2 + k_4C_2^2 \quad (8c)$$

derived from (1–4), where $I'(x,t)$ is given by (6) and[18] $\alpha_i = \epsilon_i \ln 10$. (A complete list of symbols is given in Table II.) The (nonreactive) azobenzene must be accounted for because it absorbs light; in the later stages of the reaction, when the initial azide has been largely consumed, the more weakly absorbing azobenzene accounts for the major part of the light absorption. Finally, secondary photolysis of the triplet nitrene to 1-azacyclohepta-1,2,4,6-tetraene[19] is neglected.

To the conservation equations (8a–c) and the expression (6, 7) for the local light intensity, initial and boundary conditions are now appended. Initial conditions appropriate to the uniform initial concentrations in the experiments of Costantino et al.[2] are

$$C_1(x,0) = C_{10} \qquad C_2(x,0) = C_3(x,0) = 0 \quad (9a\text{–}c)$$

where C_{10} is the initial concentration of phenyl azide. For im-

Table II. List of Symbols

$A(x,t)$	absorbance; see (7)
A_0	absorbance defined in connection with (5), following ref 2
$B(z,\tau)$	nondimensional concentration of PhN_3, C_1/C_{10}
$B_1(\tau)$	nondimensional amount of PhN_3, integrated over entire cell; see (17)
$C_i(x,t)$	dimensional concentration of species i
C_{10}	dimensional initial concentration of PhN_3
D_i	diffusion coefficient of species i
$E(z,\tau)$	nondimensional concentration of PhN, C_2/C_{10}
E_{ss}	steady-state value of E; see (19)
F	fraction of incident light absorbed within 0.27 mm of front optical wall in experiments of ref 2
G	nondimensional incident intensity, $\Phi_1 I_0 L/(D_1 C_{10})$
$H(z,\tau)$	nondimensional concentration of PhN=NPh, C_3/C_{10}
i	species number: *1*, PhN_3; *2*, PhN; *3*, PhN=NPh
$I'(x,t)$	dimensional light intensity, in photons per unit area per unit time
I_0'	dimensional incident light intensity
I_0	product of I_0' and illuminated area (4 mm × 1 mm in experiments of ref 2)
I_{abs}	nominal rate of light absorption in experiments of ref 2, $I_0(1 - 10^{-A_0})/V_0$; see (5) et seq.
k_i	rate constant for reaction i (i = 2, 3, 4)
L	length of reaction cell along optical path
$L_{diff,1}$	characteristic diffusion length based on 25-s time scale and diffusion coefficient of PhN_3
N_0	Avogadro's number
P	nondimensional parameter proportional to initial azide concentration, $k_3L^2C_{10}/D_1$
r_i	k_i/k_3 (i = 2, 4)
R_i	local rate of the ith reaction (i = 1, 2, 3)
t	dimensional time
$t_{diff,1}$	characteristic diffusion time for replenishment of PhN_3 in experiments of ref 2, on the basis of 1-mm width of illuminated zone
t_f	typical time of an experiment in ref 2 (25 s)
t_{irr}	irradiation times in experiments of ref 2; see Table I
$u(\tau)$, $v(\tau)$	nondimensional functions defined by (20) in terms of B and H; see also (14b)
$u'(\tau)$, $v'(\tau)$	derivatives of u and v with respect to τ
V_0	nominal irradiated solution volume in experiments of ref 2; see (5) et seq.
x	dimensional coordinate along optical path
z	nondimensional coordinate along optical path, x/L
α_i	$\epsilon_i \ln 10$
β_i	ratio of diffusivities, D_i/D_1 (i = 2, 3)
γ	initial absorbance, $\alpha_1 C_{10} L$
ϵ_i	molar absorptivity of species i
σ	α_3/α_1
τ	nondimensional time, tD_1/L^2
τ_{max}	time at which the maximum value of ϕ_{-PhN_3} is attained
ϕ_{N_2}	quantum yield of appearance of N_2
ϕ_{-PhN_3}	quantum yield of disappearance of PhN_3; see (14b)
ϕ_{max}	maximum value attained by ϕ_{-PhN_3}; see (21)
Φ_1	quantum yield for the initiation reaction (1)

(16) Reid, R. C.; Prausnitz, J. M.; Sherwood, T. K. *The Properties of Liquids and Gases*, 3rd ed.; McGraw-Hill: New York, 1977. These three correlations give values of D_1 equal to (3.04, 2.97, and 2.97) × 10^{-5} $cm^2\ s^{-1}$, respectively.

(17) Pearlstein, A. J. *J. Phys. Chem.* **1985**, *89*, 1054–1058.

(18) Calvert, J. G.; Pitts, J. N. *Photochemistry*; Wiley: New York, 1966; p 21.

(19) Chapman, O. L.; Le Roux, J. P. *J. Am. Chem. Soc.* **1978**, *100*, 282–285.

permeable cuvette walls, we have

$$\frac{\partial C_i(0,t)}{\partial x} = \frac{\partial C_i(L,t)}{\partial x} = 0 \qquad i = 1\text{–}3 \qquad (10a,b)$$

where L is the thickness of the cuvette in the direction parallel to the incident light beam.

It is convenient to nondimensionalize (6–10) in order to reduce the number of parameters upon which the solution depends. To this end, we define the nondimensional independent

$$\tau = D_1 t/L^2 \qquad z = x/L$$

and dependent

$$B = C_1/C_{10} \qquad E = C_2/C_{10} \qquad H = C_3/C_{10}$$

variables, along with the nondimensional parameters

$$\sigma = \alpha_3/\alpha_1 \qquad \beta_2 = D_2/D_1 \qquad \beta_3 = D_3/D_1$$

$$\gamma = \alpha_1 C_{10} L \qquad P = k_3 L^2 C_{10}/D_1 \qquad G = \Phi_1 I_0' L/(D_1 C_{10})$$

$$r_2 = k_2/k_3 \qquad r_4 = k_4/k_3$$

so that (6–10) can be rewritten as

$$\frac{\partial B}{\partial \tau} = \frac{\partial^2 B}{\partial z^2} - \gamma G B \exp\left[-\gamma \int_0^z (B + \sigma H)\, dy\right] - P(r_2 + 1)BE \qquad (11a)$$

$$\frac{\partial E}{\partial \tau} = \beta_2 \frac{\partial^2 E}{\partial z^2} + \gamma G B \exp\left[-\gamma \int_0^z (B + \sigma H)\, dy\right] + P(r_2 - 1)BE - 2Pr_4E^2 \qquad (11b)$$

$$\frac{\partial H}{\partial \tau} = \beta_3 \frac{\partial^2 H}{\partial z^2} + PBE + Pr_4E^2 \qquad (11c)$$

subject to the initial

$$B(z,0) = 1 \qquad E(z,0) = H(z,0) = 0 \qquad (12a\text{–}c)$$

and boundary

$$\frac{\partial B(0,\tau)}{\partial z} = \frac{\partial B(1,\tau)}{\partial z} = \frac{\partial E(0,\tau)}{\partial z} = \frac{\partial E(1,\tau)}{\partial z} = \frac{\partial H(0,\tau)}{\partial z} = \frac{\partial H(1,\tau)}{\partial z} = 0 \qquad (13a\text{–}f)$$

conditions. Equations 11–13 constitute an initial boundary value problem for a nonlinear system of integro-partial differential equations. They will be used to compute time-dependent concentration profiles for the azide, nitrene, and azobenzene, as well as the integrated quantum yield of disappearance of phenyl azide

$$\phi_{\text{-PhN}_3} = \frac{\text{moles of phenyl azide decomposed}}{\text{einsteins absorbed}} \qquad (14a)$$

Equation 14a is the fundamental definition of the quantum yield and involves no assumptions about the kinetics, light absorption, or uniformity of the reactants or other absorbing species. It can be written in dimensionless form as

$$\phi_{\text{-PhN}_3}(\tau) = \frac{\Phi_1}{G} \frac{1 - \int_0^1 B(z,\tau)\, dz}{\tau - \int_0^\tau \exp\left[-\gamma \int_0^1 [B(z,s) + \sigma H(z,s)]\, dz\right] ds} \qquad (14b)$$

Here, (14b) is the time-averaged (rather than instantaneous) quantum yield that would be determined experimentally according to (14a), and it differs from the expression of Costantino et al.[2] (their eq 5) in that it accounts for the spatial dependence of the concentration variables and does not assume a constant optical thickness during the photolysis. The latter of these assumptions would become untenable at the large conversions considered in our analysis, thus requiring use of the less restrictive expression (14b). (Note that the conversions reported by Costantino et al.[2] do not exceed 3%.)

Analytical Results

The mathematical model (11–13) is highly nonlinear and is unlikely to possess a closed-form solution. The inclusion of diffusion precludes solution by the methods discussed by Sheats et al.[20] Thus, the primary investigation of its properties will be conducted numerically (vide infra). In this section, we discuss some analytical properties of the solution of (11–13), with particular reference to the behavior of $\phi_{\text{-PhN}_3}$.

We begin by noting that $\phi_{\text{-PhN}_3}$ is a function of time and from (14b) must have the asymptotic behavior

$$\phi_{\text{-PhN}_3} \rightarrow \frac{\Phi_1}{G(1 - e^{-\gamma\sigma/2})\tau} \qquad (15)$$

as $\tau \rightarrow \infty$, owing to the fact that all of the reactant is ultimately consumed, while light is absorbed indefinitely by azobenzene. Application of L'Hôpital's rule to (14b) shows that

$$\phi_{\text{-PhN}_3}(0) = \Phi_1 \qquad (16a)$$

This result may also be deduced from the mechanism (1–4), from which it is seen that at values of τ sufficiently small for essentially none of the nitrene to have reacted via (2) and (3), the number of phenyl azide molecules decomposed will be equal to Φ_1 multiplied by the number of photons absorbed.

Repeated application of L'Hôpital's rule to (14b) yields

$$\phi_{\text{-PhN}_3}(\tau) = \Phi_1\{1 + \tfrac{1}{2}[\gamma^2 + P(r_2 + 1)]\tau + \ldots\} \qquad (16b)$$

where the higher order terms grow rapidly in complexity. We observe from (16b) that $\phi_{\text{-PhN}_3}$ initially increases above Φ_1. This is due to the fact that the first nitrene molecules created will react (if k_2 and k_3 are not both zero) with azide by reactions 2 and 3, thus leading to an initial increase of the effective quantum yield.

At intermediate times, the numerical simulations will show that $\phi_{\text{-PhN}_3}(\tau)$ may rapidly increase to values greatly in excess of unity, or reach a modest maximum (slightly in excess of Φ_1), before decaying asymptotically to zero according to (15).

Estimation of the Second-Order Rate Constants

Since the relative importance of the termination reaction (4) is maximized when the nitrene species is highly localized, an upper bound on the quantum yield can be computed by assuming uniform light absorption, initiation, and [PhN]. With these assumptions, Costantino et al.[2] estimated the branching/termination ratio $r_2 = k_2/k_3 = 1.0038$ from a least-squares fit of their deoxygenated data. From this, they obtained a relationship between k_2 and k_4 of the form $k_2 \simeq (0.1k_4)^{1/2}$. (A corrected least-squares fit of the same form to their data gives $k_2^2/k_4 = 10.5\ \text{M}^{-1}\ \text{s}^{-1}$.) If a steady-state approximation is made for [PhN], then it can readily be seen that r_2 must exceed unity if $\phi_{\text{-PhN}_3}$ is to exceed $4\Phi_1$.

As we shall see, the kinetics of the overall process depend on r_2 (the branching/termination ratio) and r_4 (the ratio of the rate constants for the two azobenzene-forming reactions). In light of the nonhomogeneity of the experiments of Costantino et al., these ratios are subject to considerable uncertainty. Thus, the simulations described in the following text were performed for several sets of bimolecular rate constants less than or equal to the diffusion-limited values.[21]

Numerical Solution

The numerical solution of the initial boundary value problem (11–13) was accomplished by using second-order accurate difference approximations to discretize the spatial derivatives in (11a–c) and (13a–f) and Simpson's rule to approximate the integrals. The time derivatives were approximated by a simple explicit difference scheme. These techniques are described in standard textbooks.[22]

(20) Sheats, J. R.; Diamond, J. J.; Smith, J. M. *J. Phys. Chem.* **1988**, *92*, 4922–4938.

(21) Benson, S. W. *Foundations of Chemical Kinetics*; McGraw-Hill: New York, 1960.

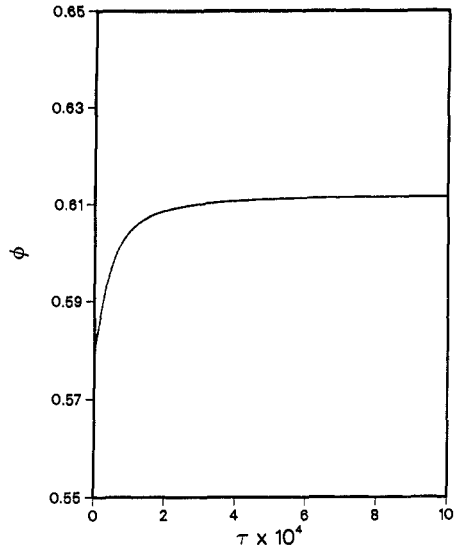

Figure 1. Computation of $\phi_{\text{-PhN}_3}$ for $r_2 = 3.5$, $r_4 = 10^5$, $k_3 = 10^3$ M^{-1} s^{-1}, $I_0 = 6.48 \times 10^{14}$ photons s^{-1}, and $C_{10} = 10^{-5}$ M. The dimensional time corresponding to $\tau = 10^{-3}$ is $t = \tau L^2/D_1 = 33.4$ s.

This simple scheme was selected because it was easy to implement and the explicit time differencing could be very efficiently vectorized for the Cray X-MP/48 and the local SCS-40 minisupercomputer. In a fully implicit scheme, the integro-differential character of the coupled equations (11a–c) would lead, at each time step, to the inversion of a block triangular matrix, a process that cannot be vectorized as easily. Stability of the numerical scheme employed here typically requires much smaller time steps than are allowed with implicit time differencing. The combined CPU time for all of the runs reported here was sufficiently small to justify a posteriori our choice of algorithm.

Accuracy was monitored at each time step in each simulation by performing a mass balance. The quantity

$$\int_0^1 [B(z,\tau) + E(z,\tau) + 2H(z,\tau)]\, dz$$

which is initially unity was conserved to within an absolute error of 10^{-7} during each run. For representative cases, accuracy was assessed by halving the time step and spatial grid size. In no case were the concentrations or integrated quantum yield found to differ by more than 3%.

Numerical Results

In lieu of accurate estimates of the rate constants, numerical simulations have been performed for several sets of rate constants. Since the integrated concentration of the intermediate species

$$B_1(\tau) = \int_0^1 B(z,\tau)\, dz \qquad (17)$$

should probably remain fairly small at reasonable values of I_0', certain unrealistic combinations of k_2, k_3, and k_4 can be eliminated. The results presented herein were obtained in the spirit of illustrating the importance of mass transfer, absorbance, light intensity, and sampling time effects in this branched-chain photodecomposition. Quantitative modeling of the experiments of Costantino et al.[2] will have to await either a detailed treatment of their fully three-dimensional irradiation geometry (including free convection), or the performance of similar experiments in a geometry in which the light intensity and concentration distributions are one-dimensional. In all calculations, $L = 1$ cm, as in the experiments of Costantino et al.,[13] and $\Phi_1 = 0.58$. We have specified the incident light intensity I_0' in terms of the quantity I_0 reported by Costantino et al.,[2] where I_0 is the product of I_0' and the irradiated area (4 mm × 1 mm). Unless otherwise indicated, we have taken $I_0 = 6.48 \times 10^{14}$ photons s^{-1}, a value used in and typical of[13] the

(22) Mitchell, A. R. *Computational Methods in Partial Differential Equations*; Wiley: New York, 1969.

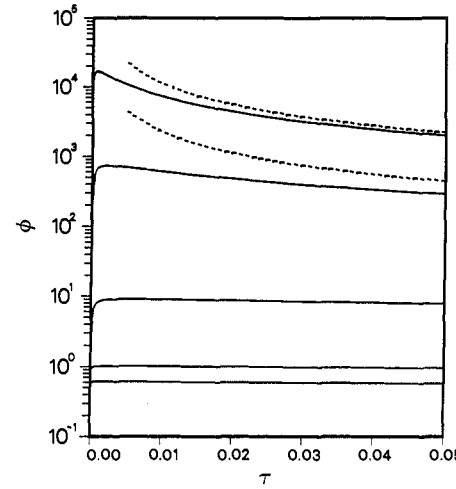

Figure 2. Computation of $\phi_{\text{-PhN}_3}$ for $r_2 = 3.5$, $r_4 = 10^5$, $k_3 = 10^3$ M^{-1} s^{-1}, and $I_0 = 6.48 \times 10^{14}$ photons s^{-1}, with different values of C_{10}. The fractional conversions at $\tau = 0.05$ are 0.44, 0.14, 0.18, 0.65, and 0.91, in order of increasing azide concentration, for $C_{10} = 10^{-5}$, 3×10^{-4}, 2×10^{-3}, 2×10^{-2}, and 10^{-1} M. (The lowest curve corresponds to the smallest value of C_{10}.) The dotted lines are the asymptotic values of $\phi_{\text{-PhN}_3}$ given by (15) for the two largest values of C_{10}.

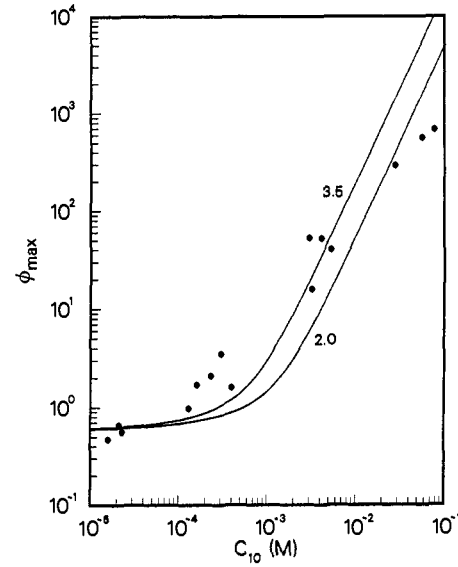

Figure 3. Solid curves show the maximum value attained by $\phi_{\text{-PhN}_3}$ as a function of C_{10} for the values of r_2 shown, with $r_4 = 10^5$, $k_3 = 10^3$ M^{-1} s^{-1}, and $I_0 = 6.48 \times 10^{14}$ photons s^{-1}. The points correspond to the quantum yields reported by Costantino et al.

experiments of Costantino et al.[2]

For an initial phenyl azide concentration of 10^{-5} M with $r_2 = 3.5$, $r_4 = 10^5$, and $k_3 = 10^3$ M^{-1} s^{-1}, Figure 1 shows that $\phi_{\text{-PhN}_3}(\tau)$ rapidly rises to ~0.61 before beginning its slow monotonic decay to zero. Figure 2 shows $\phi_{\text{-PhN}_3}(\tau)$ for a range of values of C_{10}. The rapid increase of $\phi_{\text{-PhN}_3}$ with increasing C_{10} is plainly evident. The unimodal behavior of $\phi_{\text{-PhN}_3}$ as a function of time is also clear, as is the rather strong dependence of $\phi_{\text{-PhN}_3}$ on sampling time for larger values of C_{10}. For higher concentrations, the reaction is largely completed at $\tau = 0.05$, corresponding to a dimensional time of 1670 s. For higher C_{10}, the results are in reasonably good agreement with the predicted asymptotic decay of $\phi_{\text{-PhN}_3}$ (15; shown by dotted lines). For lower values of C_{10}, the fractional conversions corresponding to $\tau = 0.05$ are much smaller, and the asymptotic limit has not been reached at the values of τ shown.

Figure 3 shows the maximum values of ϕ, defined as

$$\phi_{max} = \max_{\tau} \phi_{\text{-PhN}_3} \qquad (18)$$

for the same values of r_4 and k_3, with $r_2 = 2$ and 3.5. Also shown are the values of $\phi_{\text{-PhN}_3}$ measured by Costantino et al.[2] In light

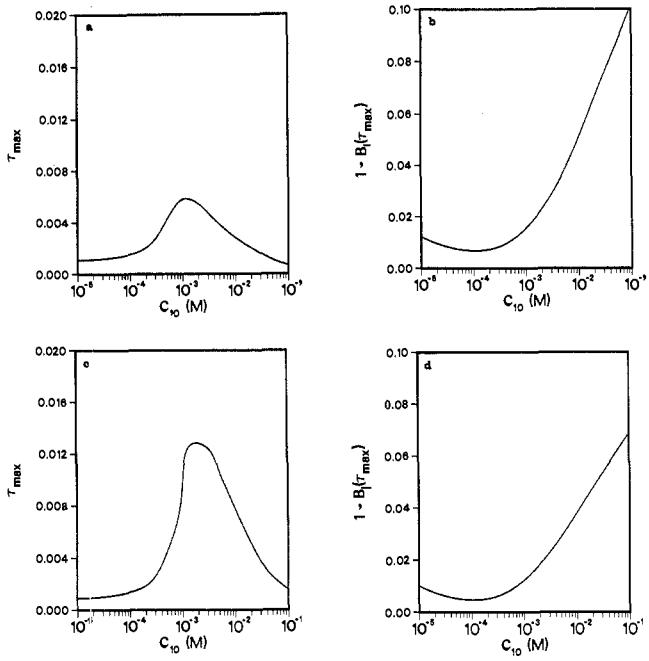

Figure 4. τ_{max} and fractional conversion as functions of C_{10}, with $r_4 = 10^5$, $k_3 = 10^3$ M^{-1} s^{-1}, and $I_0 = 6.48 \times 10^{14}$ photons s^{-1}. For $r_2 = 3.5$: (a) τ_{max}; (b) $1 - B_1(\tau_{max})$. For $r_2 = 2$: (c) τ_{max}; (d) $1 - B_1(\tau_{max})$.

of the fact that the rate constants are unknown and the measurements were not necessarily made at the times at which ϕ_{-PhN_3} reached its maximum value, the qualitative agreement is very good. That the quantum yields are uniformly lower for the smaller value of $r_2 = k_2/k_3$ is clearly due to the fact that reducing r_2 is equivalent to reducing the rate of the chain-branching reaction (2) relative to the rate of the termination step (3).

For both values of r_2, the predicted value of ϕ_{max} increases monotonically with C_{10} and is asymptotically equal to Φ_1 at small values of C_{10}. At higher concentrations, ϕ_{-PhN_3} increases as the 1.96 power of C_{10} for both values of r_2, as shown in Figure 3. That the slope of the logarithmic plot changes from zero to almost 2 is not surprising, in light of the unimolecular nature of (1), which is essentially the only reaction consuming azide at low C_{10}, and the bimolecularity of (2) and (3), which consume most of the azide at higher C_{10}. This point will be discussed at greater length in the Discussion.

For the same values of r_4 and k_3, with $r_2 = 3.5$, Figure 4a shows τ_{max}, the value of τ at which ϕ_{-PhN_3} reaches its maximum value, as a function of C_{10}. One may note that τ_{max} is a unimodal function of concentration and that its rapid rise corresponds closely to the departure of ϕ_{-PhN_3} from the low-C_{10} asymptotic value of Φ_1. The rapid decrease in τ_{max} with increasing C_{10} is associated with the very rapid decomposition of phenyl azide observed experimentally at high concentrations. Figure 4b shows the fractional conversion $(1 - B_1)$ of phenyl azide at time τ_{max}, and indicates that, at low concentrations, the peak value of ϕ_{-PhN_3} occurs at very low fractional conversions, while at higher C_{10}, ϕ_{max} occurs at higher conversions.

Figures 4c and 4d show the analogous quantities for $r_2 = 2$. Here, τ_{max} is more sharply peaked than for $r_2 = 3.5$ and is shifted to somewhat lower values of C_{10}. These results are consistent with the reduced rate of the chain-branching step (2) relative to the termination step (3) at lower r_2.

For $r_2 = 3.5$, the same values of r_4 and k_3, and a range of C_{10}, parts a–d of Figure 5 show dimensionless concentration profiles B for phenyl azide at fractional conversions of 0.05, 0.1, 0.25, 0.5, 0.75, and 0.9. At the lowest concentration ($C_{10} = 10^{-5}$ M), the profiles are almost flat, corresponding to the fact that for small values of γ (0.23 in this case) the exponential term in (11a) and (11b) is essentially constant, thus suppressing the only source of nonuniformity. Since P depends linearly on C_{10}, the remaining nonlinear term in (11a) is relatively unimportant, and the disappearance of azide is essentially first order at sufficiently low C_{10}. These results, and the prediction that $\phi_{max} = 0.61$, are consistent with the unimportance of the chain mechanism at low concentrations, as well as with the low values of ϕ_{-PhN_3} observed by Costantino et al.[2]

For $C_{10} = 3 \times 10^{-4}$ M, we have $\gamma = 6.9$, and the nonuniformity due to the exponential in (11a) is sufficient to produce a significant gradient of azide (Figure 5b). However, C_{10} is now sufficiently large for the chain mechanism to be important, as indicated by the fact that ϕ_{max} is 1.02. The phenyl azide profiles resemble a traveling wave, with the inflection point moving progressively away from the front wall of the cell. This is reminiscent of the traveling wave behavior predicted for a single unimolecular photochemical reaction in a finite reaction cell[23] and in an unbounded geometry.[24]

At still higher values of C_{10}, the nonuniformity in $[PhN_3]$ decreases, even as γ increases ($\gamma = 46$ for $C_{10} = 2 \times 10^{-3}$ M in Figure 5c, and $\gamma = 460$ for $C_{10} = 2 \times 10^{-2}$ M in Figure 5d). This rather surprising result can be explained if one considers the spatial variations of the rates of the azide-consuming reactions. For the same values of r_2, r_4, and k_3, and $C_{10} = 0.02$ M, Figure 6 shows that although the photochemical reaction (1) is highly localized near the front of the cell (note that only the front one-fiftieth of the cell is shown) virtually all of the azide consumption occurs via reactions 2 and 3, the rates of which are nearly uniform. From the near-uniformity of the combined rates of reactions 2 and 3, each of which is proportional to the nitrene concentration, it can be shown that [PhN] is also nearly uniform over virtually the entire path length. This is seen in Figure 7, in which for high values of C_{10}, the nitrene species is localized at the front boundary only at very small times. At later times, the nitrene concentration at the front wall is only slightly higher than in the remainder of the cell, even though the initiation reaction is effectively localized in a very thin layer adjacent to the front optical window.

This result is consistent with an approximate analysis in which diffusion and the time derivative of the nitrene concentration are neglected in (11b). Under this steady-state approximation, we obtain $0 = R_1 + P(r_2 - 1)BE - 2r_4PE^2$, from which it follows that the local steady-state nitrene concentration is given by

$$E_{ss} = \frac{(r_2 - 1)B}{4r_4}\left\{1 \pm \left[1 + \frac{8r_4R_1}{P(r_2 - 1)^2B^2}\right]^{1/2}\right\} \qquad (19)$$

where R_1 is the local (i.e., nonuniform) rate of the photochemical initiation.

We first note that, for $r_2 > 1$, the positive sign must be chosen on the grounds that the alternative gives $E_{ss} < 0$. Similarly, for $r_2 < 1$, we choose the negative sign. The validity of the approximation that E is steady and that nitrene diffusion can be neglected must be verified from the results. In fact, if $r_2 > 1$ and C_{10} is sufficiently large, the results show that the second term in the square brackets can be neglected in comparison to unity (as might be inferred from the small value of R_1 shown in Figure 6) and that B is effectively uniform. (Otherwise, the second term in the square brackets in (19) is not negligible in comparison to unity, and the *uniform* steady-state approximation in which R_1 is neglected compared to $R_2 + R_3$ is no longer valid.) Then, (19) reduces to $E_{ss} = (r_2 - 1)B/(2r_4)$. Hence, the only two sources of spatial variation in (19) are unimportant after a very short initial transient, and the nitrene concentration is effectively uniform, as shown in Figure 7.

Figure 8 shows $\phi_{-PhN_3}(\tau)$ for several values of I_0. The curves are approximately self-similar, and at any time the quantum yield is almost inversely proportional to I_0. The diminution of ϕ_{-PhN_3} with increasing I_0 is clearly related to the fact that the nitrene concentration increases rapidly with increasing I_0, thus leading to an increase in the rate of the biradical termination reaction (4) relative to the rate of the branching reaction (2). Hence, the proposed mechanism predicts that the chain length and quantum

(23) Terrones, G.; Pearlstein, A. J., to be submitted for publication.
(24) Terrones, G.; Fife, P. C.; Pearlstein, A. J., to be submitted for publication.

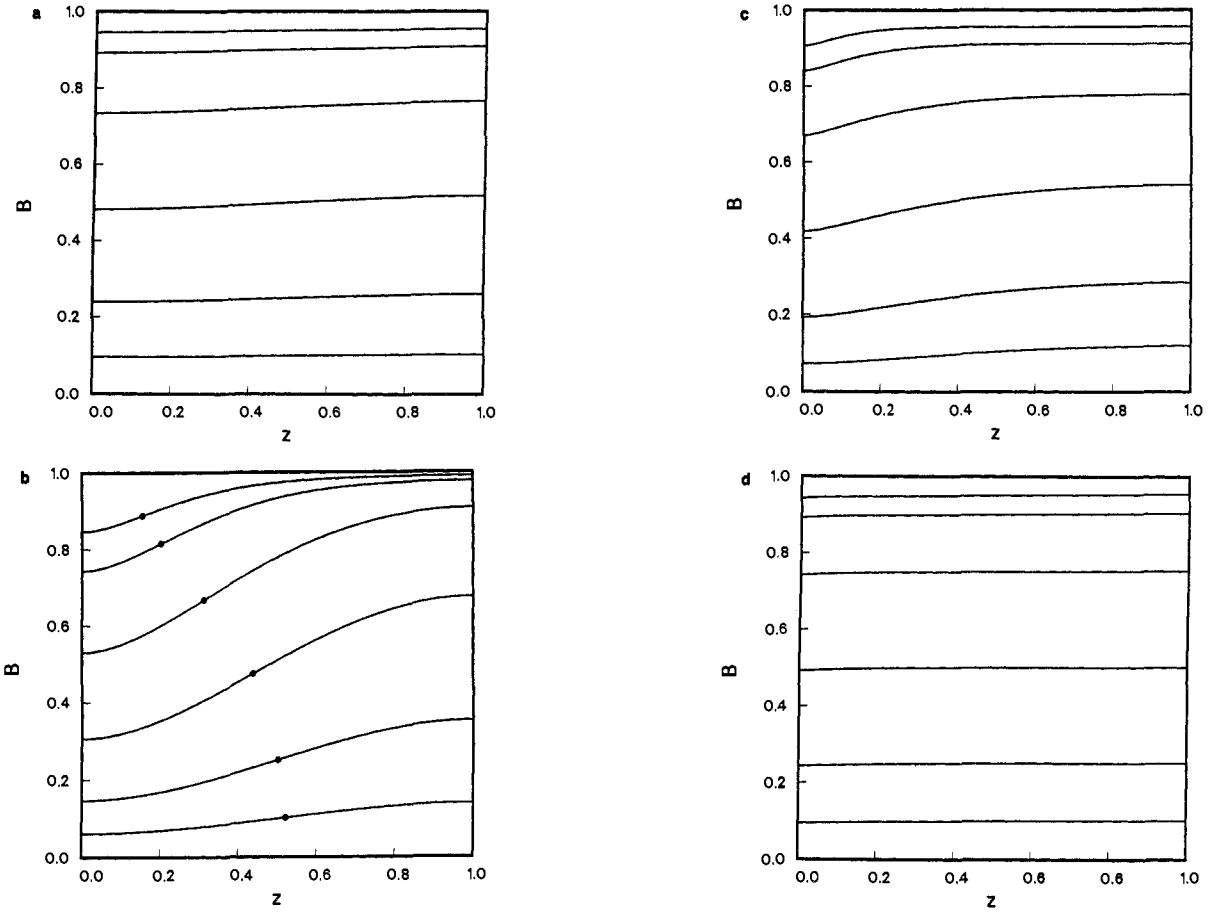

Figure 5. For $r_2 = 3.5$, $r_4 = 10^5$, $k_3 = 10^3$ M^{-1} s^{-1}, and $I_0 = 6.48 \times 10^{14}$ photons s^{-1}, the concentration profiles of PhN_3 at times corresponding to various fractional conversions ($1 - B_1$) of the azide, shown as ($1 - B_1$, τ). (a) $C_{10} = 10^{-5}$ M: (0.05, 4.487×10^{-3}), (0.10, 9.200×10^{-3}), (0.25, 2.500×10^{-2}), (0.50, 5.973×10^{-2}), (0.75, 0.1183), (0.90, 0.1952). (b) $C_{10} = 3 \times 10^{-4}$ M: (0.05, 1.654×10^{-2}), (0.10, 3.384×10^{-2}), (0.25, 9.063×10^{-2}), (0.50, 0.2056), (0.75, 0.3677), (0.90, 0.5404). At each time, the dot shows the location of the inflection point on the profile. (c) $C_{10} = 2 \times 10^{-3}$ M: (0.05, 1.234×10^{-2}), (0.10, 2.579×10^{-2}), (0.25, 7.554×10^{-2}), (0.50, 0.2122), (0.75, 0.5315), (0.90, 1.088). (d) $C_{10} = 2 \times 10^{-2}$ M: (0.05, 1.521×10^{-3}), (0.10, 3.061×10^{-3}), (0.25, 8.909×10^{-3}), (0.50, 2.643×10^{-2}), (0.75, 7.866×10^{-2}), (0.90, 0.2320).

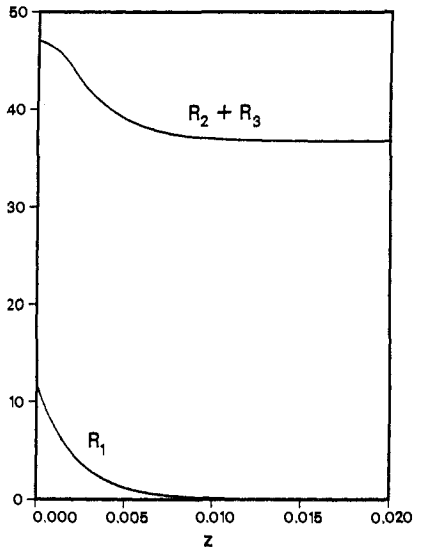

Figure 6. For $r_2 = 3.5$, $r_4 = 10^5$, $k_3 = 10^3$ M^{-1} s^{-1}, $I_0 = 6.48 \times 10^{14}$ photons s^{-1}, and $C_{10} = 2 \times 10^{-2}$ M, the spatial variation of the rates of the azide-consuming reactions at 1% conversion ($\tau = 3.872 \times 10^{-4}$). The lower curve is the rate of the photochemical reaction (1), while the upper curve shows the combined rates of reactions 2 and 3.

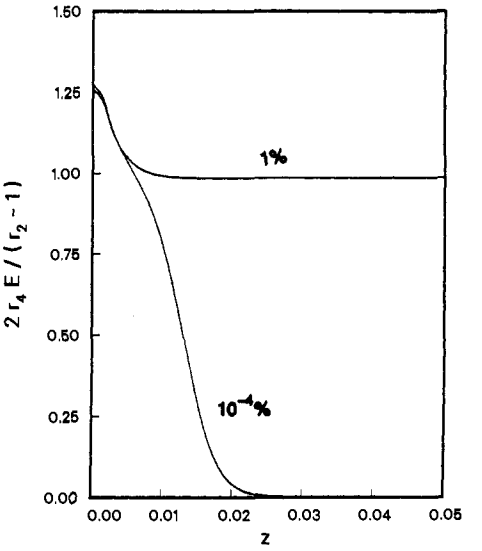

Figure 7. For $r_2 = 3.5$, $r_4 = 10^5$, $k_3 = 10^3$ M^{-1} s^{-1}, $I_0 = 6.48 \times 10^{14}$ photons s^{-1}, and $C_{10} = 2 \times 10^{-2}$ M, the upper and lower curves show the computed nitrene distributions at 1% conversion ($\tau = 3.872 \times 10^{-4}$) and 10^{-4}% conversion ($\tau = 3.6 \times 10^{-6}$), respectively.

yield will be reduced as I_0 increases.

In Figure 9, ϕ_{max} is shown as a function of I_0 for $r_2 = 3.5$ and $C_{10} = 2 \times 10^{-2}$ and 3×10^{-2} M. This plot shows a power law dependence of the form $\phi_{max} \propto I_0^{-a}$, where a asymptotically approaches unity at low I_0. (At $I_0 = 10^{15}$ photons s^{-1}, the slopes are −0.993 and −0.996 for $C_{10} = 2 \times 10^{-2}$ and 3×10^{-2} M, respectively.) At larger I_0, the magnitude of the slope begins to decrease, as required by the fact that ϕ_{-PhN_3} is bounded below by Φ_1.

Figure 10 shows that the degree of nonuniformity in the azide distribution depends not only on C_{10}, but also on the light intensity.

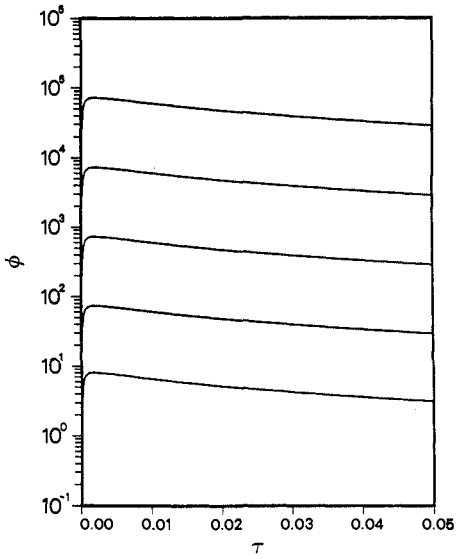

Figure 8. For $r_2 = 3.5$, $r_4 = 10^5$, $k_3 = 10^3$ M^{-1} s^{-1}, and $C_{10} = 2 \times 10^{-2}$ M, the computed time dependence of ϕ_{-PhN_3} for $I_0 = 10^n$ photons s^{-1}, with (from the top) n = 12–16.

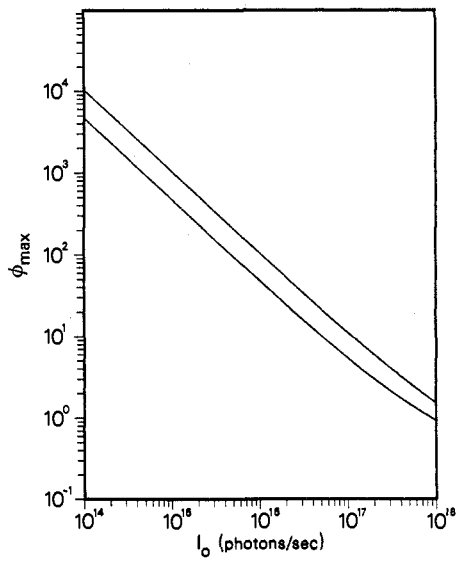

Figure 9. For $r_2 = 3.5$, $r_4 = 10^5$ and $k_3 = 10^3$ M^{-1} s^{-1}, ϕ_{max} as a function of I_0 for $C_{10} = 2 \times 10^{-2}$ M (lower curve) and 3×10^{-2} M (upper curve). At $I_0 = 10^{15}$ photons s^{-1}, the slopes are −0.993 and −0.996, respectively.

By comparison to Figure 5c, we see that a 100-fold increase in I_0 increases the nonuniformity of the azide profiles over the whole range of conversions. This reflects the fact that at sufficiently high I_0, the mechanism of Costantino et al.[2] predicts that [PhN] is sufficiently high that the biradical termination reaction (4) removes nitrene radicals at a rate in excess of the combined rates of the chain-branching and termination reactions (2) and (3). This is in turn responsible for a reduced value (0.706) of ϕ_{max}.

Discussion

Figure 3 shows the maximum values of ϕ_{-PhN_3} predicted by the model as a function of initial azide concentration, for $r_4 = 10^5$, $k_3 = 10^3$ M^{-1} s^{-1}, with $r_2 = 2$ and 3.5. The results are in good qualitative agreement with the experiments of Costantino et al.[2] The degree of quantitative agreement is consistent with the uncertainty in the rate constants, our model's exclusion of convection and diffusion into and out of the irradiated volume, and the fact that the sampling times in the experiment are unlikely to have coincided with the times at which ϕ_{-PhN_3} reached a maximum.

Recently, Liang and Schuster[9] have reinvestigated the photolysis of 3- and 4-nitrophenyl azides, for which Jenkins et al.[3] had previously found quantum yields greatly in excess of unity at high

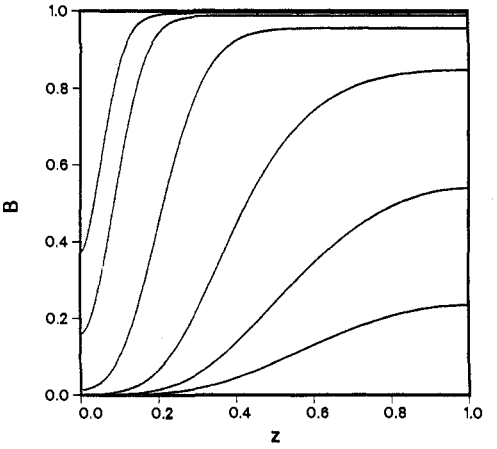

Figure 10. For $r_2 = 3.5$, $r_4 = 10^5$, $k_3 = 10^3$ M^{-1} s^{-1}, $C_{10} = 2 \times 10^{-3}$ M, and $I_0 = 6.48 \times 10^{16}$ photons s^{-1}, the concentration profiles of PhN_3 at times corresponding to various fractional conversions $(1 - B_1)$ of the azide, shown as $(1 - B_1, \tau)$: (0.05, 1.638×10^{-3}), (0.10, 3.595×10^{-3}), (0.25, 1.266×10^{-2}), (0.50, 4.604×10^{-2}), (0.75, 0.1275), (0.90, 0.2489).

values of C_{10}. At high initial azide concentrations, Liang and Schuster found quantum yields less than unity, and interpreted their experimental results in terms of a mechanism that does not include free-radical chain reactions.

In fact, both of these observations are consistent with the proposed mechanism of Costantino et al.[2] For $r_2 = 3.5$, $r_4 = 10^5$, and $k_3 = 10^3$ M^{-1} s^{-1}, Figure 8 shows that $\phi_{-PhN_3}(\tau)$ decreases approximately inversely with increasing incident light intensity for a high value of C_{10}. For the same values of r_2, r_4, and k_3, Figure 9 shows the approximately inverse dependence of ϕ_{max} on I_0 for the same values of C_{10}.

The proposed mechanism of Costantino et al.[2] indeed predicts that ϕ_{-PhN_3} should decrease as I_0 increases. This is due to the fact that as I_0 decreases, so too does the nitrene concentration, thus leading to a decrease in the importance of the biradical termination reaction (4) in comparison to the chain-branching reaction (2) and chain termination reaction (3). This argument can be made more quantitative if (14b) is rewritten as

$$\phi_{-PhN_3}(\tau) = \frac{\Phi_1}{G} \frac{u(\tau)}{v(\tau)} \tag{20}$$

and one notes that the maximum value of ϕ_{-PhN_3} occurs at $\tau = \tau_{max}$, when $u'(\tau_{max})\, v(\tau_{max}) = u(\tau_{max})\, v'(\tau_{max})$, from which it follows that

$$\phi_{max} = \frac{\Phi_1}{G} \frac{u'(\tau_{max})}{v'(\tau_{max})} \tag{21}$$

We then integrate (11a) over $0 \le z \le 1$, neglect the spatial variation of B (an approximation checked previously at high values of C_{10}), neglect the direct photochemical decomposition of azide in comparison to the rates at which it is consumed by (2) and (3) (consistent with the results of Figure 6), and finally obtain

$$\phi_{max} = \frac{k_3 L C_{10}^2}{I_0}(r_2 + 1) B(\tau_{max})\, E(\tau_{max})$$

The steady-state approximation discussed previously can then be used to eliminate $E(\tau_{max})$, yielding

$$\phi_{max} = \frac{L k_3}{2} \frac{r_2^2 - 1}{r_4} B^2(\tau_{max}) \frac{C_{10}^2}{I_0} \tag{22}$$

At high C_{10}, the quadratic dependence on C_{10} is evident from Figure 3, and the inverse dependence on I_0 is evident from Figures 8 and 9. We note the similarity between (22) and (5) if $B(\tau_{max})$ is inversely proportional to I_0.

There is indeed some experimental evidence available in the work of Costantino et al. and Liang and Schuster consistent with the predicted decrease of ϕ_{-PhN_3} with increasing I_0. For C_{10} =

1.6×10^{-4} M, Costantino et al. reported that ϕ_{-PhN_3} decreased from 1.83 to 1.57 as the incident intensity increased by a factor of 4.2. (At $C_{10} = 0.169$ M in air-saturated acetonitrile, Costantino et al. reported that ϕ_{-PhN_3} was reduced by a factor of 5.4 as I_0 was increased by a factor of 1.7.) In the experiments of Liang and Schuster, the intensity of 313-nm radiation incident on the reaction vessel from their 200-W "low power" Hg lamp was several orders of magnitude higher than that employed in the earlier work of Jenkins et al.[3] on 4-nitrophenyl azide. Thus, the low quantum yields obtained by Liang and Schuster using the 200-W Hg lamp and the even higher power 1-MW pulsed N_2 laser (which delivers about 4.5×10^{24} photons cm^{-2} s^{-1} (averaged over the 13-ns pulse duration[25]) can be reconciled with the present model. For the 1 mm × 4 mm irradiated zone in the experiments of Costantino et al., this corresponds to $I_0 = 1.8 \times 10^{23}$ photons s^{-1}. From Figure 8, it is evident that the reaction mechanism (1–4) will predict a low value of ϕ_{-PhN_3} (close to Φ_1) for this high intensity. The present work thus provides a resolution of two apparently conflicting sets of experimental results in terms of a single mechanism.

The results of our simulations of the photolysis of phenyl azide show that interpretation of the experiments of Costantino et al.[2] may be seriously complicated by the high absorbances employed and that mass transfer limitations may lead to highly nonuniform concentration profiles (e.g., Figure 5b). A remarkable result is that the concentration profile of phenyl azide may undergo a transition from nearly uniform to highly nonuniform and back to nearly uniform as the initial azide concentration (and hence the absorbance) is increased. At high initial azide concentrations, the rate of the chain-branching step can be nearly uniform (Figure 6), even though the initiation rate is highly nonuniform. Moreover, the branched-chain nature of the proposed mechanism leads to a significant dependence of the apparent quantum yield on the time at which the reaction cell is sampled.

The governing conservation equations employed in our simulations explicitly exclude convective transport. In fact, due to the nonuniform nature of the light absorption (and subsequent heat generation via various nonradiative decay processes), buoyancy-driven thermal convection *must* occur in the experiments of Costantino et al., in which the absorbing fluid is irradiated from the side.[17] The extent to which this motion has a significant effect on the progress of the reaction is less clear. When the temperature gradient is localized near the front optical window, it will likely give rise to an upwardly directed (thermal) boundary layer flow on the front window of the cell. Of course, the fluid density also depends on composition, so that when the reaction proceeds nonuniformly (e.g., Figure 5b) and the dependence of density on concentration is sufficiently strong, the direction of the flow might actually be downward if the partial molar density of the product is higher than the density of the bulk fluid. In either case, this boundary layer flow will have the effect of replenishing the depleted fluid in the irradiated volume with fresh fluid from below (or above) and will also continuously sweep the light-absorbing product (azobenzene) from the irradiated volume. Thus, convection will increase the quantum yield to an extent that depends on the size of the Grasshof number (a measure of the ratio of buoyancy forces to viscous forces in the fluid) and other nondimensional parameters.

(25) Schuster, G. B. Private communication.

Conclusion

Our analysis shows that the absorbances of the reacting solutions employed in the experiments of Costantino et al.[2] have important consequences for the mechanism proposed. In particular, we predict a strong effect of sampling time on the apparent quantum yields. Nonetheless, the results of Costantino et al. are in generally good qualitative agreement with their proposed mechanism. However, because of these effects, little quantitative confidence can be placed in the (corrected) derived relationship $k_2^2/k_4 = 10.5$ M^{-1} s^{-1} between the bimolecular rate constants for the chain-branching and biradical termination steps. For similar reasons, we have reservations about their estimate that $r_2 = k_2/k_3 \simeq 1$.

Our analysis also shows that the seemingly contradictory results of Liang and Schuster[9] and Costantino et al.[2] can be reconciled in terms of the mechanism proposed by the latter authors if one properly accounts for the dependence of the apparent quantum yield on the incident light intensity.

More generally, the results demonstrate the importance of accounting for spatial nonuniformity and the time dependence of apparent quantum yields in photoinitiated chain decompositions (or other photochemical reactions) conducted at high absorbances.

Acknowledgment. We acknowledge helpful discussions and correspondence with H. W. Richter, G. B. Schuster, and W. H. Waddell and suggestions by anonymous reviewers. This work was supported in part by Unocal and the matching funds provisions of the National Science Foundation Presidential Young Investigator Program, through NSF Grant MSM-8451157. Some of the computing was performed with use of the resources of the NSF San Diego Supercomputer Center, access to which is gratefully acknowledged.

Registry No. PhN_3, 622-37-7; acetonitrile, 75-05-8.